Global Journal of Engineering Science and Research Management

EXPERIMENTAL AND FINITE ELEMENT ANALYSIS OF TORSIONAL BEHAVIOR OF INTERNALLY-STRENGTHENED RC BOX BEAMS USING STEEL BRACINGS TECHNIQUE

Muhammad Hussein Abdallah*, Dr. Ali Hameed Aziz
* Postgraduate student (M.Sc.), Civil Engineering Department, Al-Mustansiriayah University, Iraq
Prof. Dr., Civil Engineering Department, Al-Mustansiriayah University, Iraq

ABSTRACT

In the present paper, experimental and finite element analysis was performed to investigate the torsional behavior of reinforced self-compacting concrete box beams. The experimental program consists of cast and testing of five simply supported beam specimens under the effect of pure torsion. All beam specimens have dimensions of (2100x300x300mm) for length; width and depth respectively. Each beam was reinforced by (2ϕ12mm) longitudinal bars at the top and bottom, while, the transverse reinforcement consists of (ϕ8@65mm) stirrups at ends and (ϕ8@130mm) stirrups at the mid. The first beam specimen was non-strengthened (reference beam), while, the other beam specimens were strengthened by (three X-Type), (five X-Type), (five XW-Type) and (five K-Type) steel bracing respectively. Tests results show that the ultimate torque moment increased by about (34%), (59%), (72%) and (82%) for beam specimens strengthened by (three X-Type), (five X-Type), (five XW-Type) and (five K-Type) steel bracing respectively, in comparison with the reference beam.

To study more thoroughly the structural behavior of the tested specimens, numerical analysis was performed by 3-D nonlinear finite element procedure using ANSYS (Version-15) software. The analysis results show that the torque-angle of twist response, torque-warping response and crack pattern are in good agreement with the experimental results.

INTRODUCTION

Reinforced concrete members in a structure may be subjected to axial forces, shear forces, bending moments, torque, or a combination of these effects. The torsional failure may be considered one of the more dangerous failure type than other types of failure because of its uncontrolled failure and does not give an attention before failure. Diagonal cracks occurred when the torsion stress exceeds the ultimate torsion strength of concrete; therefore, to improve the torsional capacity, there are several traditional ways such as increasing the compressive strength of concrete, adding an additional transverse and longitudinal reinforcement. Design codes are generally based on one of two major approaches, the space truss analogy and the skew bending theory. New revisions that were adopted in ACI Building Code 318 (1995; 1999; 2002; 2005, 2008, 2011) replaced the design method that was used before with one based on thin walled tube truss analogy [1]. The purpose of the modifications was to simplify the design procedures carried out to study the behavior of concrete members subjected to torsion or shear forces.

Box beams are referred to as thin-walled structures because of their cross-sectional dimensions. These types of beams have been used widely in bridge construction, because of the structural advantages of closed BOX section. However, prediction of the response of box beam bridges involves many difficulties caused by the complex interaction of the individual structural effects [2].

Structurally, each element is designed to meet a certain requirements of service load. When the applied load increase, the elements must be meet new requirements. In certain situations, it may be not possible to replace the existing element that does not satisfy the new structural requirements by a new one, or may be replacing a new element as alternate to old one is not economically feasible solution as well as substitutions of all structure. Therefore, in order to avert failure of these elements at torsional load, adequate reinforcement (longitudinal and transverse), repairing and strengthening are required. Strengthening of concrete members to resist torsional

Global Journal of Engineering Science and Research Management

stresses may be done by one of the following techniques: (i) increasing the member cross-sectional area, (ii) adding transverse reinforcement, (iii) using externally bonded steel plates, (iv) applying an axial load to the member by external prestressing [3,4]. Reinforced concrete sections under torsional stresses and externally strengthened by CFRP are interested in several research [5,6]. Beams reinforced internally with GFRP reinforcements under pure torsion are also interested [7]. Moreover, strengthening by adding internal concrete diaphragms, in transverse direction, for prestressed and non-prestressed self-compacting concrete box beams was investigated [8, 9].

Sometimes, it's difficult to perform an external strengthening for box beams (girders) due to beam's geometry or system complexity. Therefore, the needs for internal strengthening by using simple systems are arise. One of the best ways is placing (inserting) an internal steel bracing inside the hollow core of the box beams. Actually, the concept of transverse steel bracing is not new idea in steel structures. This idea is widely used in straight steel box girders and horizontally curved box girders to resist torsional stresses. The new idea, in the present paper, is utilization of this concept to torsional strengthening of the reinforced self-compacting concrete box beams by placing inside the box. In this research, three bracing systems were used with reinforced SCC box beams and compared their behavior under pure torsion.

EXPERIMENTAL WORK
Experimental program
The experimental program consists of cast and test of five large-scale SCC box beam specimens as well as a series of tests on construction materials and control specimens (cubes, cylinders and prisms) to evaluate the mechanical properties of fresh and hardened concrete. All beams have dimensions of (2100x300x300mm) for length, width and depth respectively. Since, the box beams can be design directly according to ACI 318-M14 code [1], the longitudinal and transverse reinforcement were calculated based on code requirement for torsion. Each beam was reinforced by (2ϕ12mm) bars at the top and bottom, while, the transverse reinforcement consists of (ϕ8@65mm) stirrups at the edges and (ϕ8@130mm) stirrups at the middle third. The first beam is non-strengthened beam specimen (reference beam), while, the other beam specimens were strengthened by (three X-Type), (five X-Type), (five XW-Type) and (five K-Type) steel bracing respectively. The longitudinal reinforcement, transverse reinforcement, dimensions of beams specimens, type and compressive strength of concrete, and load location will be keeps constant throughout the study. Description and details of tested beam specimens are reported and presented in Table. 1 and Figure (1) and (2).

Table 1. Description and Details of Beam Specimens

Item	Beam Designation	Dimensions (mm)			No. of Bracing	Bracing Type
		L	W	H		
1	B-R*	2100	300	300	None	-
2	B-3.0X				Three	X-Type
	B-5.0X				Five	
3	B-5.0XW				Five	XW-Type
4	B-5.0K				Five	K-Type

*Reference Beam

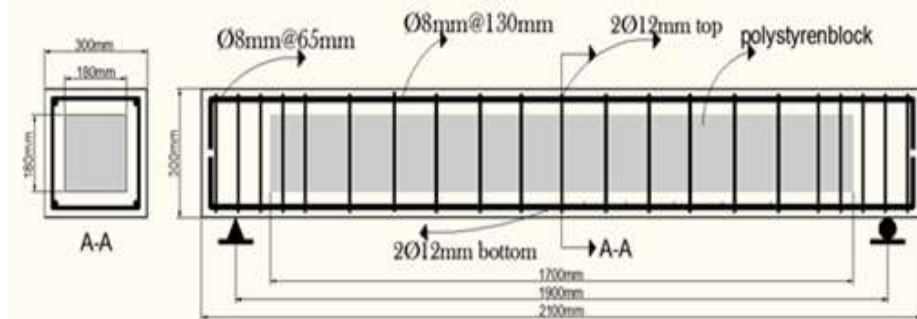Global Journal of Engineering Science and Research Management

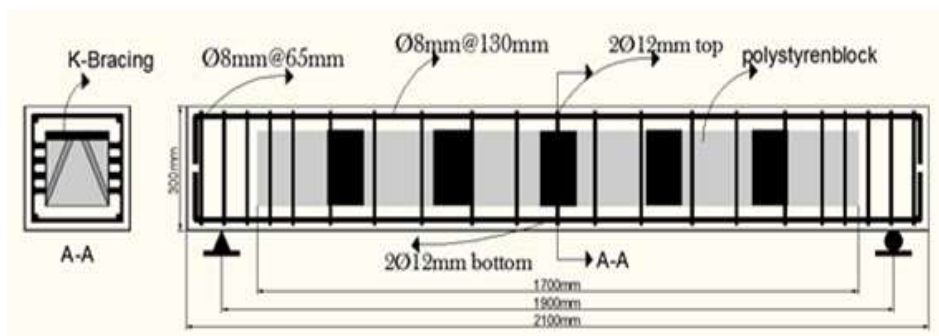*Figure. 1 Description and Details of Beam Specimens (B-R*)*

Figure. 2 Description and Details of Beam Specimens (B-5.0K)

Materials
In manufacturing the beam specimens, properties and description of the used materials as well as properties of steel bars are presented in Tables. 2 and 3 respectively. Concrete mix proportions are presented in Table. 4.

Table 2. Properties of Construction Materials

Material	Descriptions
Cement	Ordinary Portland Cement (Type I)
Sand	Natural sand from Al-Ukhaidher region with maximum size of (4.75mm)
Gravel	Crushed gravel of maximum size (12mm)
Limestone powder	Fine limestone powder (locally named as Al-Gubra) of Jordanian origin
Silica Fume	Silica fume is a highly reactive material; this type of silica fume is produced by the Sika company.
Superplasticizer	Glenium 51 manufactured by BASF Construction Chemicals, Jordan
Water	Clean tap water

Table 3. Properties of Steel Bars

$D_{nominal}$ (mm)	$D_{measured}$ (mm)	Bar Type	f_y (MPa)	f_u (MPa)	E_s^{**} (GPa)	Elongation %
8	7.9	Deformed	465	632	200	16
12	11.8	Deformed	496	644	200	16

**ACI 318-M14

Global Journal of Engineering Science and Research Management

Table 4. Mix Proportions Details

Cement (kg/m³)	Sand (kg/m³)	Gravel (kg/m³)	Limestone (kg/m³)	Silica Fume (kg/m³)	Water (liter/m³)	Superplasticizer (Liter/m³)
450	780	980	130	30	190	10

Molds and Polystyrene Blocks

Wooden molds with (18mm) thickness plywood were used to cast beam specimens. Each mold consists of a bed and two movable sides, these sides have been fixed together by screws to form the required shape. Polystyrene blocks are used to form the hollow inside the beam because of it is lightweight and its facility to configure with the required dimensions. For all tested beams, beyond the cells (at the ends), whole beam section was solid concrete, as shown in Figure (3).

Figure. 3 The mold and Steel Reinforced with Polystyrene Blocks

Test Measurement and Instrumentation

Hydraulic universal testing machine of (3000 kN) capacity was used to test the beam and control specimens. A simple method was used to estimate the angle of twist by using dial gauge attached to the bottom fiber of the end of the beam at a point (30 mm) from the end of the longitudinal axis of the beam. The dial gauge (0.01mm/div. accuracy) recorded the vertical deflection to find the twist angle in radians at every load stage. Also, two dial gauges were attached at the edges of each beam to measure the longitudinal elongation, as shown in Figure (4). The strains in steel bracing, steel bars and concrete were measured by means of strain gauges attached in different locations, as shown in Table. 5 and Figure (5).

Figure. 4 Dial Gauges Locations

Figure. 5 Strain Gauges in Steel bars, Steel Bracing and Concrete

Table 5. Strain Gauges Locations

Gauge No.	Location
1	At Stirrup (280mm) Away From The Edge
2	At Longitudinal Steel Bars (200mm Distance From The Edge)
3	At Stirrup (Mid-Span)
4	At Longitudinal Steel Bars (Mid-Span)
5	At Intermediate Steel Bracings (Mid-Span)
6	At Steel Bracings (At Edge)
7	At the top face of Beam (concrete), (Mid-Span and 40mm Distance From Right side)
8	At the top face of Beam (concrete), (Mid-Span and 40mm Distance From Left side)

Beam Specimens Test Procedure
Before testing, positions of supports, applied load, strain gauges and dial gauges were marked. The beam specimens were placed on the testing machine and adjusted so that the centerline, supports, point loads, strain gauges and dial gauges were fixed in their correct or proper locations. The surfaces (faces) of beam specimens were painted with slightly white color for monitoring the concrete cracks pattern and to "capture" first crack easily. While placing the specimens in the testing machine, care should be taken to ensure that loading is at the end of the steel arm. The steel girder of (250 mm) deep and (2500 mm) long was used to transmit the loads from the center of the universal machine to the two arms to produce pure torsion to the tested beams. The loads are applied symmetrically. During application of load to the beam, single point load is applied to the top of steel arm and is transferred as pure torque to the top of the beam, loading is continued until severe cracking of the beam occurs. The frame used in testing consists of two large steel clamps which work as arms for applied torque with separated faces to connect them over the sample by large bolts, where four bolts are used for each arm. High carbon steel plate is used to manufacture the frame with 20 mm in thickness and bolted by four 24 mm diameter bolts to prevent torque. Arm length is maximum 600 mm were applied loading of 500 mm and these points measured a way to the beam center. In order to get pure torsion, the center of support should coincide with the center of the moment arm, as shown in Figure (6).

Figure. 6 Beam Specimen Setup and Loading Arrangement

Global Journal of Engineering Science and Research Management

Properties of Fresh Concrete
To check the self-compacting concrete, four tests to evaluate filling-ability, segregation resistance and passing-ability are made. Table. 6 shows the test methods, test results and SCC requirements according to **EFNARC** [10].

Table 6. Tests Results of Fresh SCC

Test	Property	Test Result	EFNARC
Slump Flow (mm)	Filling ability	800	650-800
T_{50} (sec)		2.88	2.0-5.0
V-funnel (sec)	Segregation resistance	8.43	6.0-12
L-BOX	Passing ability	1.0	0.8-1.0

Properties of Hardened Concrete
A series of tests were carried out to determine the compressive strength, splitting tensile strength, modulus of rupture and modulus of elasticity of the concrete. Average of three (150x150x150mm) cube specimens and three (150x300mm) cylinders are used in every mix to determine the uniaxial compressive strength according to (ASTM C39/C39M-01) [11] and (BS 1881-116 1983) [12] specifications. The determination of the flexural strength (modulus of rupture) of SCC by the use of a simple beam (prisms) with dimensions of (500x100x100 mm) under two-point loading. The prisms were loaded at (450mm) span. The indirect tensile strength was carried out according with ASTM C496-96 [13]. (150x300mm) cylindrical specimens were used to compute splitting tensile strength of concrete. The specimens were tested at the age of 28 days. Static modulus of elasticity was carried out according to ASTM C469-02 [14]. (150x300mm) cylindrical specimens were used to compute modulus of elasticity of concrete. Tests results are collected and presented in Table. 7

Table 7. Mechanical Properties of Hardened SCC

Mix Type	Compressive Strength (MPa)		f_r (MPa)	f_t (MPa)	E_c (MPa)
	f'_c	f_{cu}			
SCC	41	47.8	3.78	3.2	29568

NUMERICAL ANALYSIS
To study more thoroughly the structural behavior of the tested beam specimens, numerical analysis, by 3-D nonlinear finite element method is performed by using ANSYS (Version-15) software. Verification is done to check the accuracy and validity of the finite element procedure. The accuracy of the finite element models is determined by ensuring that failure modes are true, the ultimate torque capacity is reasonably predicted in comparison with the experimental results and the torque-angle of twist curves are close to the experimental curves.

Element Types
Types of the elements that were used for modeling the tested beam specimens are reported and presented in Table. 8 It may be noted that, each element was used to represent a specified constituent of beams.

Table 8. Characteristics of the Selected Elements

Beam Component	Element Designation in ANSYS	Element Characteristics
Self-Compacting Concrete	SOLID-65	8-Node Brick Element (3 Translation DOF per node)
Reinforcing Bars and Steel Bracing	LINK-180	2-Node Discrete Element (3 Translation DOF per node)
Steel Plate	SOLID-181	8-Node Brick Element (3TDOF)

Real Constants, Material Properties and Parameters
The real constants are used to define the geometrical properties of the used elements such as cross-sectional area, thickness and other values. While, the material properties are used to represent the behavior and characteristics of the constitutive materials depending on mechanical tests such as modulus of elasticity, yield stress, Poisson`s ratio and stress-strain relationship. However, each of the specified type of elements has a number of fundamental parameters that are identified in the elements library of ANSYS. The values of those element parameters are needed for similar representation of each tested beam as they are used in approximating the elements of real constants and material properties. Elements property parameters are reported in Table. 9

Table 9. Property Parameters of Adopted Elements

Element	Parameter	Description					Value		
Solid 65	fc'	Compressive strength (MPa)					-1		
	f_t	Tensile strength (MPa)					4		
	*βo	Open shear transfer coefficient					0.3		
	*βc	Close shear transfer coefficient					0.6		
	Ec	Young's modulus of Elasticity (MPa)					29568		
	υ	Poisson's ratio					0.2		
	Description of strain-stress relationship for concrete (SOLID 65)**								
	Stress (MPa)	0	12.6	14.74	26.92	35.25	39.91	41	41
	Strain	0	0.000413	0.0005	0.001	0.0015	0.002	0.002757	0.003
	Parameter	**Description**					**Value**		
Link-180	A_b	Cross section Area (mm^2)		Main (φ12mm)			113		
				Stirrups (φ8mm)			50.26		
	f_y	Yield Strength (MPa)		(φ12mm) bar			472		
				(φ8mm) bar			580		
Link-180 and Solid-181	Es and E_t	Modulus of elasticity and strain hardening modulus (MPa)		Es			200000		
				E_t			0		
	υ	Poisson's ratio					0.3		

* It may be noticed that these value is selected after convergence study to prevent the divergence of models.
** These values were calculated from theoretical equations [16].

Modeling and Meshing of Concrete
The first step of modeling of the beam specimens includes creation of blocks of the concrete volume; the concrete volume is formed by pinpointing key-points of one side edge of the concrete block, then creating lines between these key-points to form the area, then forming by extruding these areas in the third dimension. After identifying the volumes, the finite element analysis needs meshing of the model whereby, the model is divided into a number of small elements, to obtain good consequences. By taking the advantage of the symmetry of both, beam's geometry and loading, half of the entire model beam was used for finite element analysis, Figure (7). This approach reduces computational time and computer disk space requirements significantly. To obtain good results, the mesh was set up such that square or rectangular elements were formed.
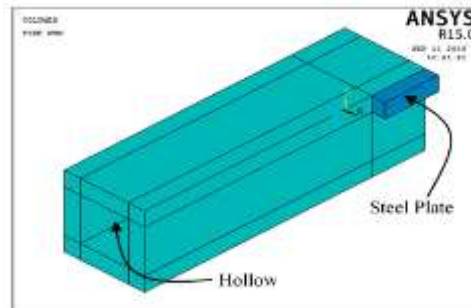
Figure.7 The Selected Half of Control Beam Used in the Analysis

Since a half of the beam is being modeled, the dimensions of the adopted model were (1050x300x300mm) for length, depth and width respectively. The origin point was assumed to be coinciding with the one corners of the cross-section for the modeled beams. Steel plates with dimensions of (200x60x50 mm) and located at the opposite loading is used to create couple in one end as shown in Figure (8).
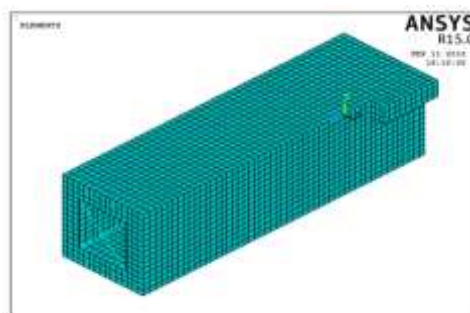

Figure.8 Modeling and Meshing of Concrete and Steel Plate

Since the volumes of steel plates and concrete are modeled separately, the model needed to glue the volumes together. To obtain good results from the concrete element (Solid-65), the use of a rectangular or square mesh is recommended. The volume of steel plate and concrete meshing is done by utilized sweep command. This properly sets the width and length of elements in the steel plates to be consistent with the elements and nodes in the concrete portions of the model. Overall mesh of concrete and steel plate volumes are shown in Figure (8).

Modeling of Steel Reinforcing Bars
In the present study, the steel reinforcements (tensile, compressive, and stirrups) were represented by using 2-node discrete representation (LINK-180 in ANSYS) and included within the properties of 8-node concrete brick elements. The reinforcement is assumed to be capable of transmitting axial forces only, and perfect bond is assumed to exist between the concrete and the reinforcing bars. To provide the perfect bond, the link element for the steel reinforcing bar was connected between nodes of each adjacent concrete solid element, so the two materials share the same nodes. Figure (9) shows the reinforcement representation in ANSYS.
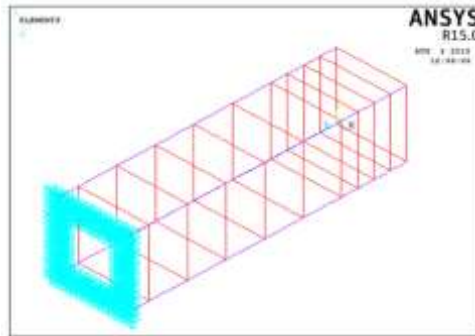
Global Journal of Engineering Science and Research Management

Figure.9 Modeling of Longitudinal and Transverse Steel Bars

Modeling of Steel Bracing
In the present study, three types of steel bracing (X-Bracing, XW-Bracing and K-Bracing) were represented by using 2-node discrete representation (LINK-180 in ANSYS) and included within the properties of 8-node concrete brick elements. To provide full bond, the plates of the steel bracing was connected with concrete solid element without using interface elements (contact elements), so the two materials share the same nodes. This assumption is considered true due to fact that the steel plates (of steel bracing) are confined inside of the BOX of the BOX beams and experimentally it is fixed with concrete by shear connecters (studs). Figure (10) shows the representation of steel plates and steel bracing in ANSYS.
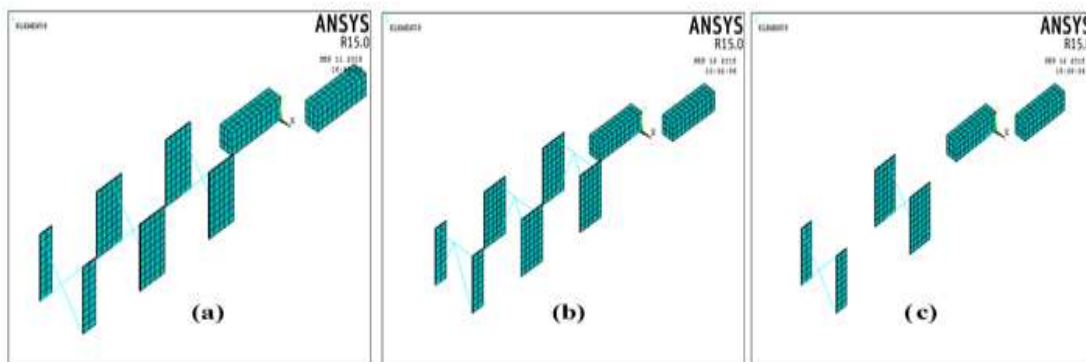
Figure .10 Modeling of Steel Bracing and Steel Plate (a) B-5.0X,
(b) B-5.0K, (c) B-3.0X

Loading and Boundary Conditions
Displacement boundary conditions are needed to constrain the model to get a good solution. To certify that the model acts the same way as the experimental specimens, boundary conditions need to be applied at points of symmetry, and where the supports and loadings exist. To simulate the fixed boundary condition at the plane of symmetry, all nodes were restrained ($U_x=U_y=U_z$) as shown in Figure (11).
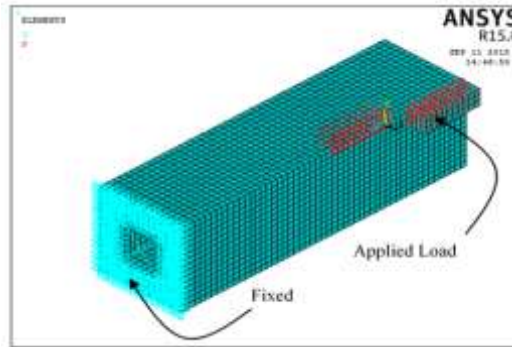
Figure.11 Loading and Boundary Conditions

The external load was applied on a steel plate; thus, the external applied load was represented by the equivalent nodal forces on the nodes of the same place of plate. Therefore, the equivalent force at each node on the plate was (1/2) of the actual force applied per nodes number. The applied load is divided into load steps and done incrementally up to failure (based on Newton-Raphson technique). At a certain stages in the analysis, load step size is varied from large (at points of linearity in the response) to small (when cracking and steel yielding occurred). The analysis is assumed to be done when the load reached its last step of loading and the phrase (solution is done!) is appeared in software screen. Otherwise, the failure is assumed to be occurred when the solution, for a minimum load is diverging and the models have a large deflection (rigid body motion).

RESULTS AND DISCUSSION
Failure Mechanism
The progress of cracks provided useful information regarding the failure mechanism of tested specimens. It is found that all the tested beam specimens were failed in torsion. The first crack of all specimens were occurred at the mid span and increased gradually. When the torque moment was increased, cracks appeared on each side and finally took the spiral shape. Figure (12) shows the failure modes for all tested beam specimens. All beam specimens were failed by extensive diagonal concrete crack (torsional spiral cracks). For reference beam specimen (B-R), due to the weakness of box section, the cracks spread in an entire beam length (un-strengthened zone) and with increasing in cracks number, the failure occurred at the mid span. For beam specimens which strengthened by steel bracing, the cracks spread with smaller number and develop more slowly in strengthened zone (bracing zones) because the transverse bracing prevented the increment of the crack's width. Also, the failure position of beam specimens took place between steel bracing intervals

Figure. 12 Mode of Failure of Tested Beams

Global Journal of Engineering Science and Research Management

Ultimate Torque Capacity

Table.11 shows the comparison between the ultimate torque of the experimental (tested) beams, $(T_u)_{EXP}$, and final torque from the finite element models, $(T_u)_{FEM}$. The final loads for the finite element models are the last applied load steps before the solution starts to diverge due to numerous cracks and large deformations (strains or angle of twisting). Comparing with the experimental results, all the finite element models show relatively large capacity at the ultimate stage. It can be observed that, there is a simulation between the finite element analysis and the experimental results of about (90-93%) for ultimate load capacity (T_u) and these ratios are considered reasonable and accepted.

Table 11. Numerical and Experimental Results

Beam Designation	T_u (kN)		Θ (Rad)		Warping (mm)		T_u (%)	θ (Rad)	Warp. (%)
	EXP.	FEM	EXP.	FEM	EXP.	FEM			
B-R	25.125	23.50	0.0212	0.0180	2.55	1.90	6.90	17.70	34.21
B-3.0X	33.750	31.75	0.0141	0.0138	2.00	1.75	6.20	2.17	14.28
B-5.0X	40.000	37.25	0.0152	0.0135	1.70	1.60	7.38	12.60	6.25
B- .0XW	43.125	39.00	0.0145	0.1400	1.53	1.36	10.50	3.57	12.50
B-5.0K	45.625	42.75	0.0140	0.0139	1.42	1.30	6.70	0.72	9.23

Torque-Angle of Twist Relationship

To study the general behavior of finite element models, torque-angle of twist plots at the end of the span near the loaded arms were represent. The angle of twist was measured by vertical displacment at end of beams (at the edge of the bottom face of the beams) in y-direction (Uy). The torque versus angle of twist, which obtained from the numerical study together with the experimental plots are presented and compared in Figures (13) to (15). In general, it can be noted from the torque-angle of twist plots that the finite element analyses are agree well with the experimental results throughout the entire range of behavior.
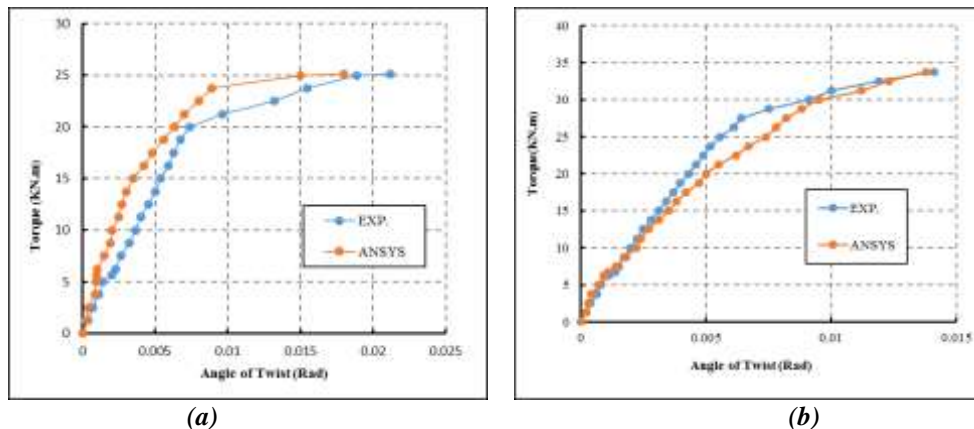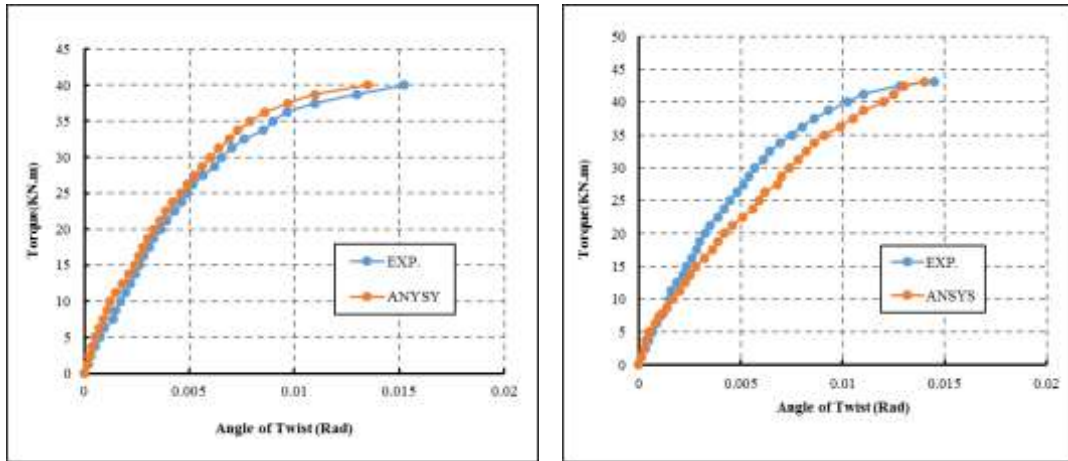

(a)   *(b)*

Figure.13 Torque-Angle of Twist (a) Model (B-R) (b) Model (B-3.0X)

Global Journal of Engineering Science and Research Management

| (a) | (b) |

Figure.14 Torque-Angle of Twist (a) Model (B-5.0X) (b) Model (B-5.0XW)
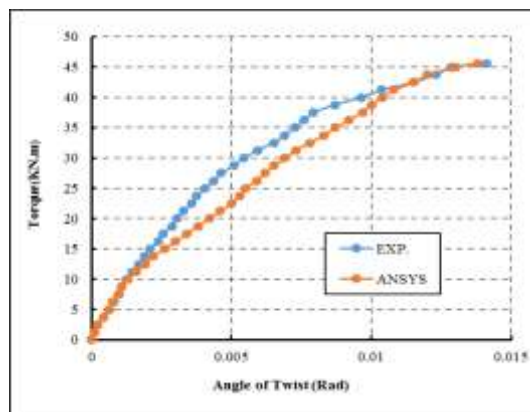

Figure.15 Torque-Angle of Twist for Model (B-5.0K)

Torque-Warping (Longitudinal Elongation) Relationship
To study the general behavior of finite element models, torque- longitudinal elongation plots at the end of the beam (at the side face of the beams) in z-direction. The torque versus longitudinal elongation, which obtained from the numerical study together with the experimental plots are presentea and compared in figures (16) to (18). In general, it can be noted from the Torque-Longitudinal Elongation plots that the finite element analyses are agree well with the experimental results throughout the entire range of behavior.
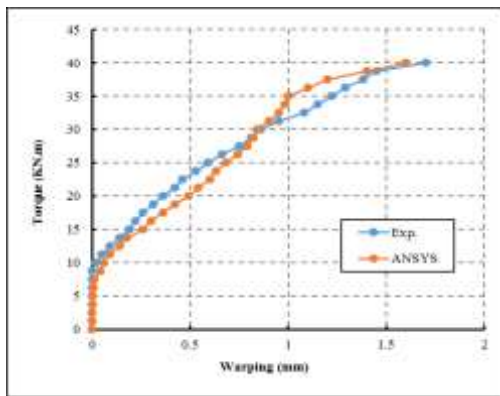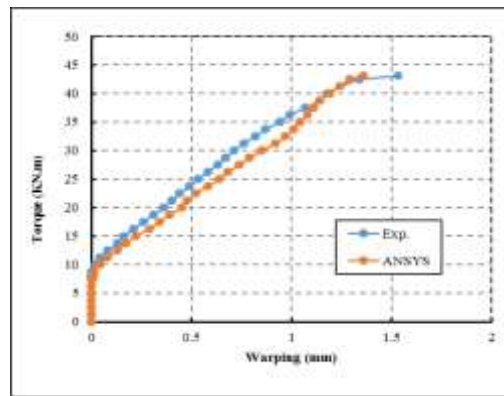
Global Journal of Engineering Science and Research Management
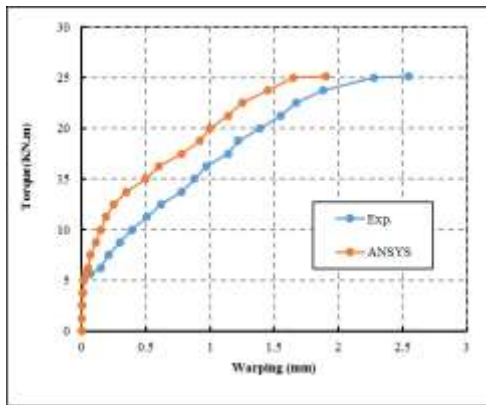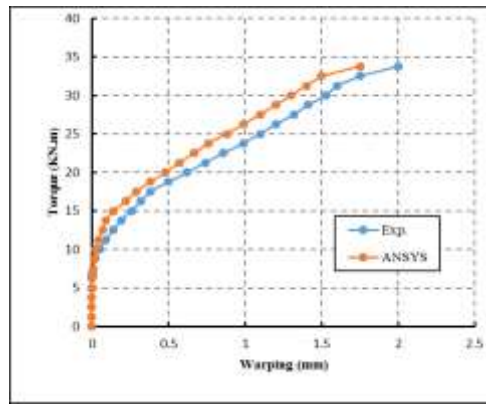
(a)   *(b)*

Figure.16 Torque- Warping Behavior (a) Model (B-R) (b) Model (B-3.0X)

(a)   *(b)*

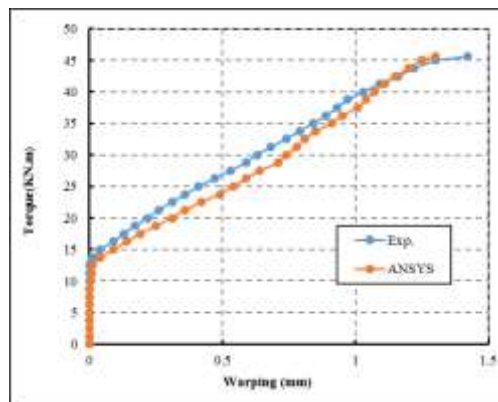**Figure.17 Torque-Warping Behavior (a) Model (B-5.0X) (b) Model (B-5.0XW)**

Figure.18 Torque-Warping Behavior for Model (B-5.0K)

Deformed Shape
The ANSYS program records the deformed shape at each applied load step. The final deformed shapes, due to the transformed of vertical load (moment), from the finite element analysis and the failure modes of the experimental beams agree well, as shown in Figure (19) and (20).
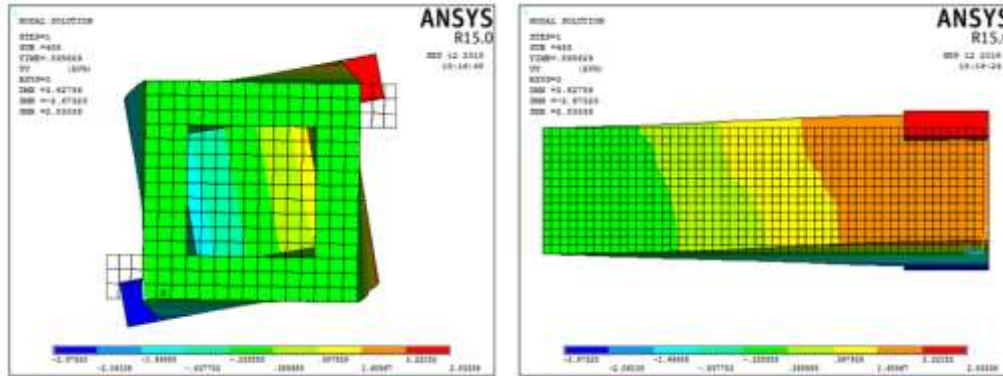
Global Journal of Engineering Science and Research Management

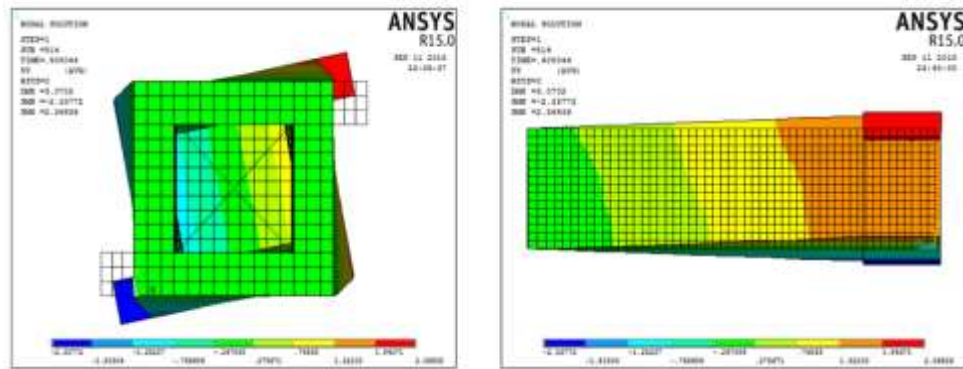*Figure.19 Deformed shape (Front and Right view) for Model (B-R)*

Figure.20 Deformed shape (Front and Right view) for Model (B-5.0XW)

Crack Patterns
The ANSYS program records the crack pattern at each applied load step. There is a good agreement between the finite element analysis and the experimental response for the beams crack patterns as shown in Figures (21) to (23). The appearance of the cracks reflects the failure mode for the beams. The model of FEM, accurately, predicts that the tested beams are failing in torsion and predicts that the inclined cracks formed through an entire beam span. The cracks are concentrated in the mid span region and vanish towards the beam supports.
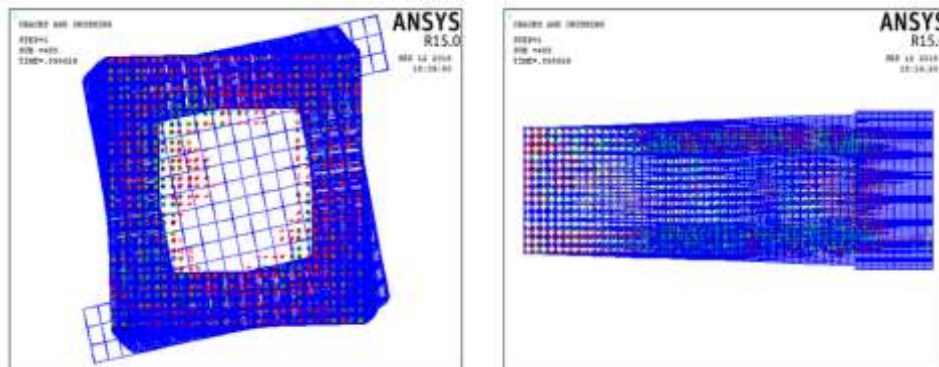

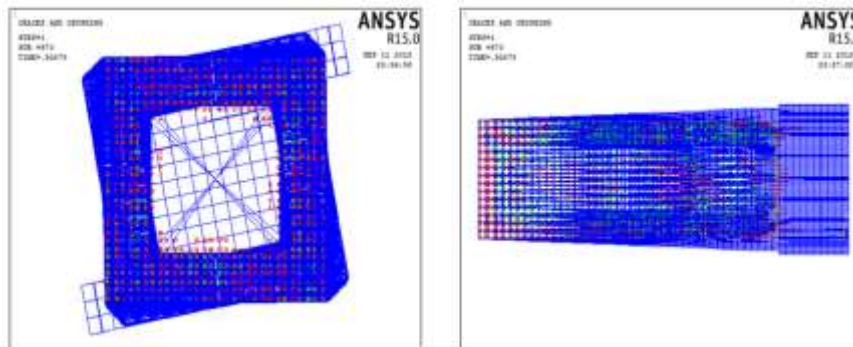*Figure.21 Crack pattern (Front and Right view) for Model (B-R)*

Global Journal of Engineering Science and Research Management

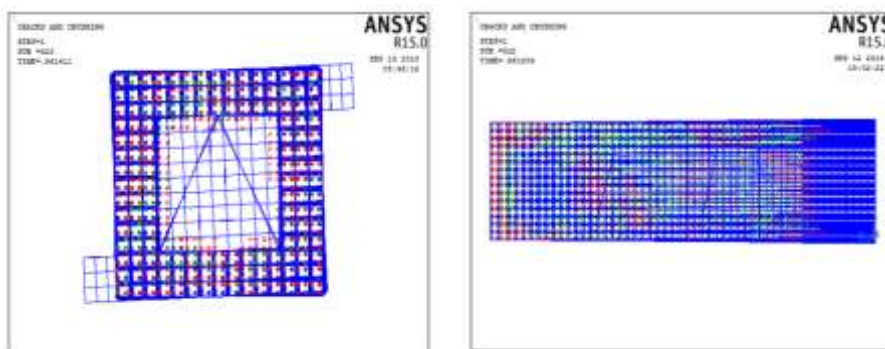*Figure.22 Crack pattern (Front and Right view) for Model (B-5.0X)*

Figure.23 Crack pattern (Front and Right view) for Model (B-5.0K)

CONCLUSIONS

Experimental work Results

1-The adopted technique (strengthening by internal steel bracings) seems to be simple and more effective to increase section torsional capacity.

2- For beam specimens who strengthened internally by three and five X-type steel bracing, the ultimate torque moment increases for about (34% and 59 %) respectively, also, the angle of twist decreases for about (18.8% and 30.365%) respectively. From the other side, the longitudinal elongation decreases for about (21.56% and 33.33%) respectively.

3- For beam specimens who strengthened internally by five XW-type steel bracing, the ultimate torque moment increases for about (72%), also, the angle of twist decreases for about (32.42%). From the other side, the longitudinal elongation decreases for about (40%).

4- For beam specimens who strengthened internally five K-type steel bracing, the ultimate torque moment increases for about (82%), also, the angle of twist decreases for about (35.6%). From the other side, the longitudinal elongation decreases for about (48.87%).

5- The K-type steel bracing is more efficient than the XW-type, also, the XW-type steel bracing is more efficient than the X-type steel bracing.

Numerical Analysis Results

1-The failure mechanism of reinforced concrete beams was investigated well by using the adopted finite element models. The ultimate torque predicted were very close to the ultimate torque measured in experimental tests. It can be observed that, there is agreement between the numerical (finite element) analysis and the experimental results of about (93%) for ultimate torque capacity and this ratio is considered reasonable and accepted.

2-The crack patterns obtained for numerical (finite element) modeled beams are similar to the crack pattern observed in experimental work

3-The angle of twist-torque curves and Warping- torque curves for numerical (finite element) modeled beams

results has a good agreement with the experimental curves.

REFERENCES

1. ACI Committee 318, "Building Code Requirements for Structural Concrete (ACI 318M-14)   and Commentary (ACI 318RM-14)", American Concrete Institute, Farmington Hills, MI, USA, pp.519.
2. Lars, J.R., "Plastic Behavior of Deformable Reinforced Concrete BOX Sections under Eccentric Load", Ph.D. Thesis, University of Queensland, (1996).
3. MacGregor, J. G. and Ghoneim, M. G., "Design for Torsion", ACI Structural Journal, Vol. 92, No. 2, pp. 211-218, (1995).
4. Khalil, A., Etman, E., Atta, A., and Fayed, S., "Torsional Strengthening of RC BOX Beams Using External Prestressing Technique", IOSR Journal of Mechanical and Civil Engineering (IOSR-JMCE), Vol. 12, No. 2, pp. 30-41, (2015).
5. Ban, S. A., Ali, H. A. and Israa, K. M., "Strengthening of Reinforced Concrete Beams under Combined Torsion and Bending Using Carbon Fiber Reinforced Polymer Strips", The Iraqi Journal for Mechanical and Material Engineering, Vol. 12, No. 4, pp. 754-769, (2012).
6. Abeer A. M., Allawi A. A., and Chai H. K., "Theoretical Study on Torsional Strengthening of Multi-cell RC BOX Girders", World Academy of Science, Engineering and Technology, International Journal of Civil Science and Engineering Vol. 7, No. 2, (2013).
7. Prabaghar, A. and Kumaran, G., "Theoretical Study on the Behavior of Rectangular Concrete Beams Reinforced Internally with GFRP Reinforcements under Pure Torsion", International Journal of Civil and Structural Engineering, Vol. 2, No. 2, (2011).
8. Ali, H. A. and Oday, H. H., " Torsional Strengthening of Prestressed Self Compacting Concrete BOX Beams Using Internal Transverse Concrete Diaphragms Technique", Journal of Engineering and Sustainable Development, Vol. 21 , No. 5, (2017)
9. Ali, H. A. and Oday, H. H., "Torsional Strength Evaluation of Reinforced SCC BOX Beams Strengthened Internally by Opened and Closed Transverse Concrete Diaphragms ", Proceeding of 3rd International Conference on Buildings, Construction and Environmental Engineering-Egypt, 23-25 Oct. (2017).
10. 10- EFNARC, "Specification and Guidelines for Self-Compacting Concrete", Association House, 99 West Street, Farnham, Surrey GU9 7EN, UK, pp.21, February 2002, Available at (www.efnarc.org).
11. ASTM C39-96, "Test Method for Compressive Strength of Cylindrical Concrete Specimens", (ASTM C39-96), American Society for Testing and Materials, (1996).
12. BS 1881-116, "Method for Determination of Compressive Strength of Concrete Cubes", British Standards Institute, London, (1983).
13. ASTM C496-96, "Standard Test Method for Splitting Tensile Strength of Cylindrical Concrete Specimens", (ASTM C496-96), American Society for Testing and Material, (1996).
14. ASTM C 469-02, "Standard Test Method for Static Modulus of Elasticity and Poisson's Ratio of Concrete in Compression", (ASTM C 469-02), American Society for Testing and Material, (2002).A. James and A. Lupton, "Gypsum and anhydrite in foundations of hydraulic structures," Geotechnique, vol. 28, pp. 249-272, 1978.
15. Ahmed, R. H., "Behavior of Reactive Powder R.C T-section Beams with Openings for Pure Torsion", M. Sc. Thesis, Civil Engineering, College of Engineering, Mustansiriyah University, 2016.
16. Wolanski, A.J., "flexural Behavior of Reinforced and Prestressed Concrete Beams using Finite Element Analysis", M.Sc. thesis, Marquette University, 2004.